USING FILTER BANKS TO ENHANCE IMAGES FOR FLUID LENS CAMERAS BASED ON COLOR CORRELATION

Jack Tzeng and Truong Nguyen

University of California, San Diego, Electrical and Computer Engineering
La Jolla, California 92092
Email: jatzeng@ucsd.edu and nguyent@ece.ucsd.edu

ABSTRACT

The novel field of fluid lens cameras introduces unique image processing challenges. Intended for surgical applications, these fluid optics systems have improved miniaturization over glass lenses and do not have moving parts while zooming. However, the liquid medium creates non-uniform color blur, which causes certain color planes to appear sharper than others. We propose an adapted perfect reconstruction filter bank that uses high frequency sub-bands of sharp color planes to improve blurred color planes. The approach is refined by adjusting the decomposition level based on limited channel information. This paper primarily considers the use of a sharp green color plane to improve a blurred blue color plane. More generally, these methods could improve the red color plane as well as any system with high edge correlation between two images.

Index Terms— Biomedical image processing, image enhancement, image reconstruction, image color analysis.

1. INTRODUCTION

Lo invented a fluid lens camera system that, over glass lens systems, has a smaller size and does not have moving parts while zooming [1, 2]. Modifying a reconstruction filter bank, we attempt to deal with the new image processing challenges of this system. Primarily, the fluid lens system affects different color wavelengths non-uniformly (Fig. 1). The design places the CMOS sensor to focus the green color, leaving the red color and blue color out of focus.

Previous research on image deblurring can be classified into linear and non-linear methods. Reviews of these methods can be found in [3, 4]. Some approaches apply glass lens ideas [5, 6] such as Lucy-Richardson deconvolution [7, 8] and Weiner deconvolution [9].

This paper adapts a method used in image demosaicking [10] by modifying a reconstruction filter bank. The algorithm enhances the sharpness of the blue image by fusing edge information from the green image. By adding additional levels of decomposition, this algorithm performs approximately 5 dB better than traditional methods. The proposed method requires only limited channel knowledge in order to optimize the filter bank design.

2. NOTATION

The following is a short list of notations:

This work is supported by a grant from UCSD VonLieBig Foundation and the UCSD Chancellor's Fellowship in San Diego, California

(a) Green Image from the Device (b) Blue Image from the Device

Fig. 1. The device blurs different color planes differently.

$\hat{B}$	$\hat{}$ represents an estimate of B after lens blurring
$\widehat{BLH}$	Sub-band output after filtering and down-sampling $\hat{B}$ twice, an L represents a low-pass filter and an H represents a high-pass filter at each level
$\hat{B}_r$	Subscript r represents the reconstruction of $\hat{B}$
$\hat{B}_{rL}$	Subscript L represents the low frequency sub-band output of $\hat{B}_r$
$\hat{G}_{rH}$	Subscript H represents the high frequency sub-band output of $\hat{G}_r$
E_G	The error for an estimate of G

3. WAVELET SUB-BAND MESHING ALGORITHM

For most natural color images, the Red, Green, and Blue (RGB) color planes exhibit high edge correlation [10, 11]. In contrast, the shading changes between color planes. For the fluid lens system, different color planes experience different amounts of blur. This paper modifies a perfect reconstruction filter bank to improve the blue image resolution by substituting green image edge information.

A standard perfect reconstruction filter bank decomposes a signal into separate sub-bands [12], then reconstructs the original signal. The proposed system (Fig. 2) replaces the edge sub-bands of the blue image with the edge sub-bands of the green image. The blurring causes the $\widehat{BHL}$, $\widehat{BLH}$, and $\widehat{BHH}$ sub-bands. The $\widehat{BLL}$ sub-band maintains the blue shading while the $\widehat{GLH}$, $\widehat{GHL}$, and $\widehat{GHH}$ sub-bands estimate the edges. Depending on the level of blur, this algorithm uses more green information by increasing the decomposition level of the $\widehat{BLL}$ and $\widehat{GLL}$ sub-bands.

The algorithm uses a weak blue image and a strong green image:

1. Select a perfect reconstruction filter bank.

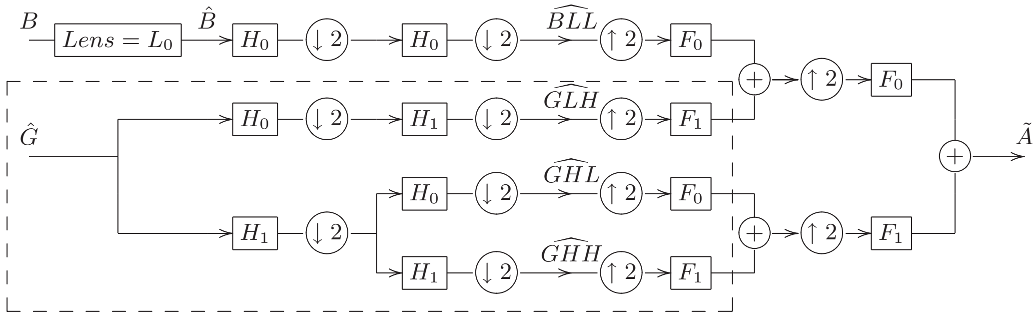

Fig. 2. Modified Reconstruction Filter Bank that takes Edges from the Green Image and Shading from the Blue Image.

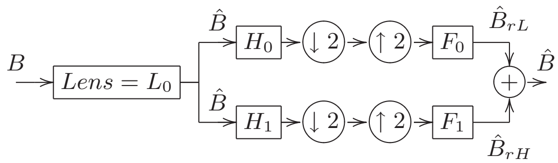

Fig. 3. Standard Perfect Reconstruction Filter Bank with Blurring.

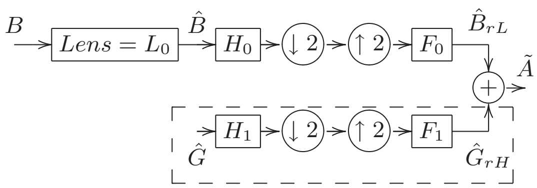

Fig. 4. One Dimensional Modified Reconstruction Filter Bank.

2. Decompose the images into four sub-bands by first filtering and down-sampling the rows, then filtering and down-sampling the columns.
3. Replace the band pass sub-bands of the blue image ($\widehat{BLH}$, $\widehat{BHL}$, $\widehat{BHH}$) with the band pass sub-bands of the green image ($\widehat{GLH}$, $\widehat{GHL}$, $\widehat{GHH}$).
4. Depending on the blur, increase the level of decomposition to further down-sample and filter the $\widehat{BLL}$ component, replacing more sub-bands with the corresponding green color sub-bands.
5. Reconstruct by up-sampling and filtering.

3.1. Analysis of the Algorithm

For clarity purposes, the analysis shows the one dimensional case, but these ideas naturally extend to the two dimensional case. Also, assume that all filters have unit gain.

In Fig. 3, $L_0(z)$ models the blurring effects of the lens on the true blue image $B(z)$ as a low-pass filter.

$$\hat{B}_{rL}(z) = \frac{1}{2}F_0(z)(H_0(z)\hat{B}(z) + H_0(-z)\hat{B}(-z)) \tag{1}$$

$$\hat{B}_{rH}(z) = \frac{1}{2}F_1(z)(H_1(z)\hat{B}(z) + H_1(-z)\hat{B}(-z)) \tag{2}$$

Modifying this filter bank, we replace $\hat{B}_{rH}(z)$ with $\hat{G}_{rH}(z)$ from the green image sub-band of Fig. 4:

$$\hat{G}_{rH}(z) = \frac{1}{2}F_1(z)(H_1(z)\hat{G}(z) + H_1(-z)\hat{G}(-z)) \tag{3}$$

In order to reconstruct the original signal B, the estimate for the higher sub-band used in reconstruction must be close to the higher sub-band of the original B signal. From the optical properties of the lens, $\hat{G}$ better estimates the edges of the original blue signal:

$$\begin{aligned} &H_1(z)\hat{G}(z) + H_1(-z)\hat{G}(-z) + E_G \\ &\quad = H_1(z)B(z) + H_1(-z)B(-z) \end{aligned} \tag{4}$$

$$\begin{aligned} &H_1(z)\hat{B}(z) + H_1(-z)\hat{B}(-z) + E_B \\ &\quad = H_1(z)B(z) + H_1(-z)B(-z) \end{aligned} \tag{5}$$

$$|E_G| \leq |E_B| \tag{6}$$

Equations (4) and (5) represent estimates of the true high-pass sub-bands of B. E_G and E_B are the errors of the two estimates. Because of edge correlation between color planes, this model assumes that the inequality (6) holds.

It can be shown that this idea leads to the following reconstruction conditions:

$$F_0(z)H_0(z)L_0(z) + F_1(z)H_1(z) = 2z^{-l} \tag{7}$$

$$F_0(z)H_0(-z)L_0(-z) + F_1(z)H_1(-z) = 0 \tag{8}$$

$$|F_1(z)E_G| = \epsilon \tag{9}$$

$H_0(z)$ and $L_0(z)$ are both low-pass filters. If $H_0(z)$ has a cutoff frequency which is lower than that of $L_0(z)$, then the following two approximations hold.

$$H_0(z)L_0(z) \approx H_0(z) \tag{10}$$

$$H_0(-z)L_0(-z) \approx H_0(-z) \tag{11}$$

Under these approximations, equations (7) and (8) match the perfect reconstruction conditions of a conventional two-channel filter bank [12]. The system output can be simplified:

$$\tilde{A}(z) = z^{-l}B(z) - \frac{1}{2}F_1(z)E_G \tag{12}$$

4. ANALYSIS OF ERROR

As stated in section 3, the derivation requires $H_0(z)$ to have a lower cutoff frequency than $L_0(z)$ so that approximations (10) and (11) hold. For a two-channel perfect reconstruction filter bank, H_0 has a transition band centered at $\omega = 0.5\pi$ [12]. The system determines $L_0(z)$ transition frequency which may be less than 0.5π. The algorithm avoids this conflict by altering the decomposition level.

The analysis shows the trade-off between the error created by using the green sub-bands versus the error created by the lens on the blue sub-bands. We show that for a large class of low-pass blurring characteristics, an optimal solution for the decomposition level, c, exists. For this class, c must be increased until the cutoff frequency of the blur falls beyond the cutoff frequency of the lowest sub-band.

Recall that $L_0(e^{j\omega})$ is the blur distortion for the blue image. Assume that it has the frequency response below:

$$L_0(e^{j\omega}) \approx \left\{ \begin{array}{rl} 1 & \text{if } |\omega| < \pi/4 \\ -3dB & \text{if } |\omega| = \pi/4 \\ 0 & \text{if } \pi/4 < |\omega| < \pi \end{array} \right\} \quad (13)$$

A two level decomposition is needed for this $L_0(e^{j\omega})$. Because the cutoff frequency of $L_0(e^{j\omega})$ is at $\pi/4$, $\widehat{BLH}$, $\widehat{BHL}$, and $\widehat{BHH}$ sub-bands poorly estimate the sub-bands of B. However, the unfiltered sub-bands of $\widehat{GLH}$, $\widehat{GHL}$, and $\widehat{GHH}$ better estimate the sub-bands of B.

It can be shown that the error E_{BLL} between BLL and $\widehat{BLL}$ simplifies to four terms:

$$\begin{aligned} P(z) &= H_0(z)B(z)(1-L_0(z)) && (14) \\ E_{BLL}(z) &= BLL(z) - \widehat{BLL}(z) && (15) \\ &= \frac{1}{4}[H_0(z^{1/2})P(z^{1/4})] \\ &\quad +\frac{1}{4}[H_0(z^{1/2})P(-z^{1/4})] \\ &\quad +\frac{1}{4}[H_0(-z^{1/2})P(jz^{1/4})] \\ &\quad +\frac{1}{4}[H_0(-z^{1/2})P(-jz^{1/4})] && (16) \end{aligned}$$

$L_0(e^{j\omega/4}) \approx 1$ when $|\omega| < \pi$, thus the first term ≈ 0. $H_0(-e^{j\omega/4}) \approx 0$ by construction, because H_0 is a low-pass filter, thus the second term ≈ 0. For the remaining two terms, $H_0(-e^{j\omega/2}) \approx 0$, because H_0 is a low-pass filter, thus the those terms ≈ 0.

This derivation assumes that $L_0 \approx 1$ if $|\omega| < \pi/4$. Consider making L_0 more general:

$$L_0(e^{j\omega}) \approx \left\{ \begin{array}{rl} 1 & \text{if } |\omega| < \omega_{-3dB} \\ -3dB & \text{if } |\omega| = \omega_{-3dB} \\ 0 & \text{if } \omega_{-3dB} < |\omega| < \pi \end{array} \right\} \quad (17)$$

In order to reduce E_{BLL}, the decomposition level, c, can be increased until $\frac{\pi}{2^c} \leq \omega_{-3dB} \leq \frac{\pi}{2^{c-1}}$. A large c means that the algorithm discards parts of the frequency spectrum which have not been corrupted by the lens. A small c means that in the low band of the frequency spectra, $0 \neq 1 - L(z)$ increasing E_{BLL}, as well as the reconstruction error.

The optical properties of the lens, blur out $\widehat{BLH}$, $\widehat{BHL}$, and $\widehat{BHH}$ and yield a high approximation error. $\widehat{GLH}$, $\widehat{GHL}$, and $\widehat{GHH}$ better estimate the edges of the original blue signal.

$$\begin{aligned} E_{GLH} &= BLH - \widehat{GLH} \\ E_{GHL} &= BHL - \widehat{GHL} \\ E_{GHH} &= BHH - \widehat{GHH} && (18) \end{aligned}$$

The terms in (18) all have smaller values than their corresponding blue sub-bands. The expression below shows the output:

$$\begin{aligned} \tilde{A}(z) &= z^{-l}B(z) - F_0(z)F_0(z^2)E_{BLL} \\ &\quad -F_0(z)F_1(z^2)E_{GLH} - F_1(z)F_0(z^2)E_{GHL} \\ &\quad -F_1(z)F_1(z^2)E_{GHH} && (19) \end{aligned}$$

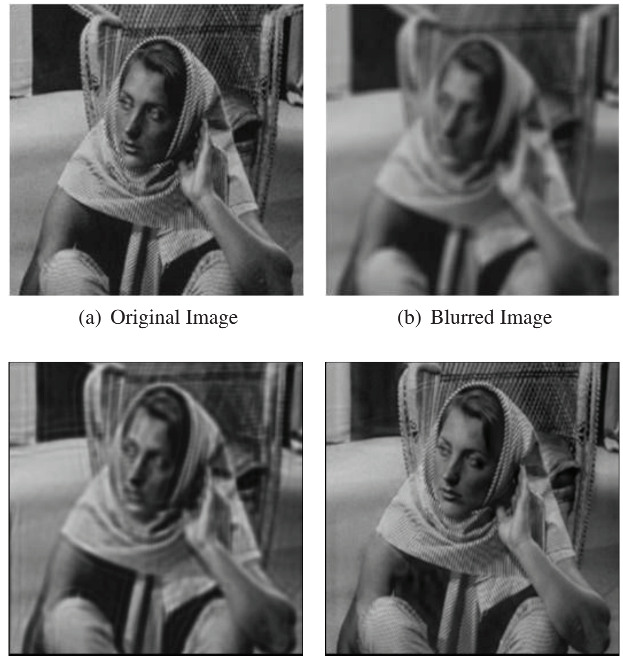

(a) Original Image (b) Blurred Image

(c) Lucy-Richardson Deconvolution (d) Proposed Algorithm

Fig. 5. This test simulates blur using a Gaussian blur kernel. The proposed algorithm yields sharper results.

As the decomposition level increases, more E_G terms appear. The decomposition level can be increased until $\frac{\pi}{2^c} \leq \omega_{-3dB} \leq \frac{\pi}{2^{c-1}}$ to minimize E_{BLL} without introducing needless E_G terms.

5. EXPERIMENTAL RESULTS

5.1. Simulated Results

Fig. 5 shows the blue image of *Barbara*, the blue color plane was blurred with a 21x21 Gaussian kernel with a standard deviation (STD) of 10. The proposed algorithm used a four levels of decomposition from modified code in [13]. Compared to the Lucy-Richardson deconvolution, this method does better.[1]

Fig. 6 compares the PSNR results of the proposed algorithm to conventional methods when the variance of a Gaussian kernel increases for a fixed window size. The proposed method has PSNR values approximately 5 dB higher than traditional method. Listed as PR, the proposed algorithm is implemented using different wavelets, such as the Daubechies wavelets [14].

5.2. Actual Image Taken From the Device

While results in section 5.1 used simulated blur kernels, the images shown in Fig. 7 use actual images from the device. The blur shown has been created by the lens and has not been simulated. The images taken were from a distance of 15 cm from the lens in a well lit laboratory setting. Additional information about the test conditions and lens functionality can be found in [1]. For this test, lens parameters were set to maximize the quality of the Green color plane at the

[1]More simulation results including video are available at: http://videoprocessing.ucsd.edu/∼jack865/ICASSP2009/

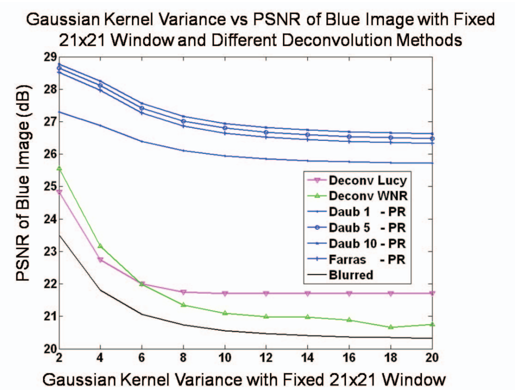

Fig. 6. Simulation to compare different deconvolution methods to the proposed (noted as PR) method.

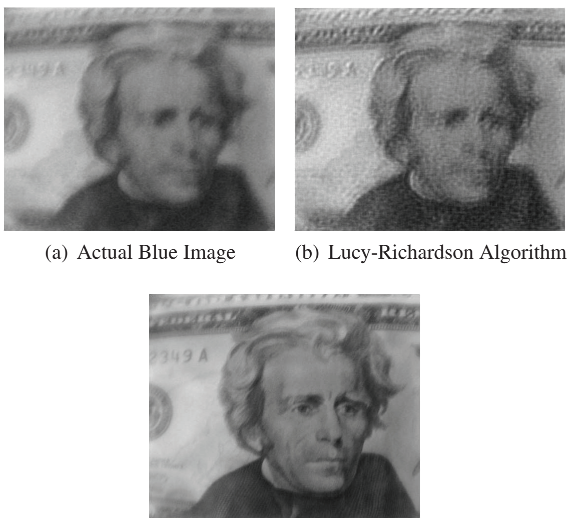

(a) Actual Blue Image (b) Lucy-Richardson Algorithm

(c) Proposed Algorithm

Fig. 7. Actual image taken from the device with blur from the fluidic lens. This experiment compares the proposed algorithm to the Lucy-Richardson Algorithm.

expense of the other color planes. In order to tune for other color planes, the curvature of the fluidic lens would need to be adjusted.

Fig. 7 compares the results of the Lucy-Richardson algorithm to the proposed algorithm. The Lucy-Richardson method results in problems with over-sharpening, however the proposed algorithm improves the image. The shading layer from the blue is preserved, and the green image edges improve the details of the proposed reconstructed images. The proposed algorithm successfully reduces the blur caused by the lens, making the resulting blue image sharper.

6. CONCLUSION

The improved design of fluid optical systems offer smaller cameras and fixed parts while zooming. However, they provide images that exhibit problems blurring. This paper proposes a wavelet subband meshing algorithm that uses edge correlation to improve color planes. The algorithm achieves gains of approximately 5 dB better than conventional methods and requires limited knowledge about the blur characteristics of the system. This work has been extended in [15], which discusses the impact of blur kernel shape and blur kernel size. It also presents color image results. This technique improves any system with high edge correlation between two images and could be used in compression and super resolution.

Acknowledgment

The authors would like to thank Frank S. Tsai and Dr. Yu-Hwa Lo for developing the fluidic lens and providing test images.

7. REFERENCES

[1] Frank S. Tsai, Sung Hwan Cho, Yu-Hwa Lo, Bob Vasko, and Jeff Vasko, “Miniaturized universal imaging device using fluidic lens,” *Optics Letters*, vol. 33, no. 3, pp. 291–293, February 2008.

[2] De-Ying Zhang, Nicole Justis, and Yu-Hwa Lo, “Integrated fluidic adaptive zoom lens,” *Optical Letters*, vol. 29, no. 24, pp. 2855–2857, 2004.

[3] Peter A. Jansson, Ed., *Deconvolution of Images and Spectra*, Academic Press, 2nd edition, 1997.

[4] Alfred S. Carasso, “Linear and nonlinear image deblurring: A documented study,” *SIAM Journal on Numerical Analysis*, vol. 36, pp. 1659–1689, 1999.

[5] Mario Bertero and Patrizia Boccacci, *Introduction to Inverse Problem in Imaging*, IOP Publishing Ltd., 1998.

[6] Mark R. Banham and Aggelos K. Katsaggelos, “Digital image restoration,” *IEEE Signal Processing Magazine*, vol. 14, no. 2, pp. 24–41, March 1997.

[7] L.B. Lucy, “An iterative technique for the rectification of observed distributions,” *The Astronomical Journal*, vol. 79, no. 6, pp. 745–754, June 1974.

[8] William Hadley Richardson, “Bayesian-based iterative method of image restoration,” *Journal of Optical Society of America*, vol. 62, no. 1, pp. 55–59, January 1972.

[9] Norbert Wiener, *Extrapolation, Interpolation, and Smoothing of Stationary Time Series*, The MIT Press, 1964.

[10] Bahadir K. Gunturk, Yucel Altunbasak, and Russell M. Mersereau, “Color plane interpolation using alternating projections,” *IEEE Transactions on Image Processing*, vol. 11, no. 9, pp. 997–1012, September 2002.

[11] James E. Adams Jr., “Interactions between color plane interpolation and other image processing functions in electronic photography,” in *SPIE*, 1995, vol. 2416.

[12] Gilbert Strang and Truong Q. Nguyen, *Wavelets and Filter Banks*, Wellesley-Cambridge Press, 1997.

[13] A. Farras Abdelnour and Ivan W. Selesnick, “Nearly symmetric orthogonal wavelet bases,” in *IEEE International Conference Acoustic, Speech, Signal Processing (ICASSP)*, May 2001, pp. 431–434.

[14] Ingrid Daubechies, *Ten Lectures on Wavelets*, Capital City Press, 1992.

[15] Jack Tzeng and Truong Q. Nguyen, “Image enhancement for fluid lens camera based on color correlation,” *IEEE Transactions on Image Processing*, 2009.